Effect of Carbon-11-Acetate Recirculation on Estimates of Myocardial Oxygen Consumption by PET

Alfred Buck, H. Georg Wolpers, Gary D. Hutchins, Vicky Savas, Thomas J. Mangner, Ngoc Nguyen, and Markus Schwaiger

Department of Internal Medicine, Division of Nuclear Medicine, University of Michigan Medical Center, Ann Arbor, Michigan

Mono- and biexponential fitting of myocardial ^{11}C-acetate kinetics does not account for the effect of recirculating ^{11}C activity following intravenous injection of the tracer. A tracer kinetic model comprising two and three compartments was developed to describe intravascular and myocardial ^{11}C-acetate kinetics defined by PET. This model approach including a correction for ^{11}C-metabolites in blood was validated by correlating the model parameter estimates with directly measured oxygen consumption (MVO$_2$) in 11 closed-chest dog experiments over a wide range of cardiac work. The model parameter k2 closely correlated with oxygen consumption (r = 0.94). This approach was subsequently applied to human studies and k2-related to rate-pressure product (PRP). In comparison to conventional monoexponential fitting of ^{11}C-acetate tissue kinetics, the model approach improved the correlation coefficients of scintigraphic MVO$_2$ estimates and PRP values from 0.61 to 0.91. Thus, analysis of myocardial ^{11}C-acetate and clearance kinetics with a tracer kinetic model corrects for recirculating ^{11}C-activity and may provide more consistent estimates of myocardial oxygen consumption.

J Nucl Med 1991; 32:1950-1957

M yocardial ^{11}C-acetate kinetics have been extensively validated as marker of myocardial oxygen consumption in animal and clinical studies (1–8). These investigations have shown that tissue ^{11}C clearance kinetics can be adequately described by monoexponential or biexponential functions. The ^{11}C clearance rate of the rapid first phase correlated closely with myocardial oxygen consumption in animals (2–7) and with the rate-pressure product as an indirect marker of myocardial oxygen consumption in man (1,8). However, the analysis of tissue time-activity curves by mono or biexponential fitting of ^{11}C tissue-clearance curves does not consider recirculating ^{11}C-acetate activity in blood. In experimental models employing

intracoronary bolus injection of the tracer, the amount of recirculating ^{11}C-acetate is negligible. In contrast, only a small fraction of the tracer is delivered to the heart during the first-pass after intravenous ^{11}C-acetate injection. Thus, the amount of recirculating ^{11}C-acetate is considerable and is expected to affect the shape of the tissue time-activity curves. Besides variation in the shape of the ^{11}C-input function, the relative contribution of ^{11}C-carbon dioxide (CO$_2$) to blood ^{11}C activity has to be considered. Since ^{11}CCO$_2$ produced by tissue metabolizing ^{11}C acetate equilibrates in plasma and red blood cells, the relative blood content of ^{11}C-acetate is expected to decrease more rapidly than the total ^{11}C activity in blood. The metabolic contamination of the ^{11}C-acetate input function may affect considerably the estimates of ^{11}C-acetate metabolism based on tracer kinetic models, if no correction of the input function is performed. We hypothesize that a model approach that considers variations of the input function and contribution of ^{11}C-metabolites is necessary for consistent scintigraphic estimation of myocardial oxygen consumption with ^{11}C-acetate. Therefore, the aim of this study was to employ compartmental models for the description of myocardial ^{11}C-acetate kinetics in the canine model and to apply this approach subsequently to clinical ^{11}C-acetate PET studies.

MATERIALS AND METHODS

Animal Studies

Eleven mongrel dogs weighing 14.5–16.4 kg were anesthetized with sodium pentobarbital (30 mg/kg body weight), incubated and ventilated with room air. Catheters were advanced through the femoral artery into the left ventricle into the descending aorta and inferior cava. For sampling of venous blood, a 5F catheter was advanced through the left or right jugular vein and placed under fluoroscopic guidance in the great coronary vein. A maximum of four experiments were performed in each animal preparation. Blood flow and oxygen demand were varied over a wide range employing pharmacological interventions described below.

Positron Emission Tomography. Imaging was performed with the University of Michigan animal PET instrument (TCC 4600 A, Cyclotron Corp.). Before tracer injection, a 10-min transmission scan was performed using an ^{18}F source for photon attenuation correction. After injection of 2–4 mCi ^{11}C-acetate as a

slow bolus (20 sec) tomographic data were recorded for 60 min as 24 frames with the following scan durations: 10 × 10, 1 × 60, 5 × 100, 3 × 180, 2 × 300, and 3 × 600 sec. Each time point (frame) was reconstructed into five transaxial slices using a 128 × 128 voxel matrix. Tissue time-activity curves were generated by placing a region of interest over the anterior wall and the values were expressed as PET cps/pixel.

Myocardial Blood Flow and Oxygen Consumption. Both regional and global left ventricular blood flow was determined prior to tracer injection with radioactive-labeled microspheres ([111]Sn, [141]Ce, [106]Ru, Dupont-NEN) and the arterial reference technique (9). Prior to the injection of the microspheres, blood samples were drawn from the left ventricle and the coronary sinus for the determination of the arteriovenous oxygen blood content. Myocardial oxygen consumption (MVO₂) was calculated as the product of oxygen extraction and blood flow and expressed as ml O_2/min/100 g myocardial tissue.

Pharmacologic Interventions. Various pharmacologic interventions were employed to alter myocardial energy demand and, hence, oxygen consumption. Propranolol (1.0–2.6 mg/kg, bolus) was used for beta receptor blockade; atropine (0.25 mg/kg, bolus) for increasing the heart rate; continuous infusions of epinephrine (0.4–1.7 μg/kg/min) and norepinephrine (0.15–0.6 μg/kg/min) as inotropic and chronotropic agents.

Human Studies

The study population comprised eight subjects, three females aged 63–68 yr and five males aged 26–58 yr. Two subjects were healthy male volunteers and six were patients with valvular heart disease, but normal left ventricular function (ejection fraction > 53%).

Positron Emission Tomography. All subjects were studied in the University of Michigan whole-body scanner (Siemens 931/08/12). At the beginning of each study a transmission scan using a Ge68/Ga68 source was performed to correct for photon attenuation. A catheter was placed into the antecubital vein and 20 mCi ^{11}C-acetate were administered as a slow bolus over approximately 20 sec. Data were recorded for 30 min after injection as 21 frames with the following scan durations: 10 × 10, 1 × 60, 5 × 100, 3 × 180 and 2 × 300 sec. A region of interest, encompassing about 3 cm³ of tissue, was placed over the anterior wall and the tissue time-activity curves calculated as mean cps/pixel.

Carbon-11-Acetate Input Function in Animal and Human Experiments. The model approach requires the exact definition of the ^{11}C-acetate input function. Since high-pressure liquid chromatography revealed that the major metabolite of ^{11}C-acetate in blood is [11]CCO₂, the true ^{11}C-acetate input function was obtained by subtracting [11]CCO₂ activity from total arterial ^{11}C activity. In the animal experiments, the time course of total ^{11}C activity concentration in arterial blood [cwtot(t)] was determined by drawing 1-ml samples from the descending aorta. Rapid sampling was performed in 5-sec intervals for the first min, then the intervals were prolonged to 20 sec until 2-min postinjection. Further samples were drawn at 3, 4, 5, 7, 10, 15, 20, 30, 40, and 60 min postinjection. An aliquot of 0.25 ml of each sample was counted in a well counter and corrected for ^{11}C decay. Cwtot(t) was then converted from the well counter units (cps/ml) to the scanner units [PET cps/vox] yielding ctot(t). For this purpose a calibration measurement with a cylindrical flood source containing [18]F (0.4 μCi/ml) was performed. In the human studies early images were used to delineate ventricular and atrial blood-pool activity and a region of interest (of approximately 0.25 cm³) was

drawn over the left atrium to determine the time course of total whole blood activity (10). The correction of total arterial ^{11}C activity for [11]CCO₂ activity was performed using a mathematical approach. For this method (floating parameter metabolite correction) the concentration of [11]CCO₂ was expressed as % total ^{11}C concentration and the continuous time course was approximated by the following exponential function:

$$a(t) = a_o (1 - \exp(-(\log 2/m) t)).\qquad\text{Eq. 1}$$

The input function ca(t) was then obtained by subtracting [11]CCO₂ activity from total arterial ^{11}C activity:

$$C_a(t) = (1 - a(t)) C_{tot}(t) \text{ [cps/ml]}\qquad\text{Eq. 2}$$

or expressed with a_o and m:

$$C_a(t) = \{1 - a_o (1 - \exp(-\log 2/m) t)\}C_{tot}(t)\qquad\text{Eq. 3}$$

Equation 3 was substituted into the equations describing tissue activity (Equations 4, 6, and 7), and a_o and m were estimated together with the kinetic parameters by the fitting routine.

To validate this approach the [11]CCO₂ concentration was measured in six animal and three human experiments, using the following method: [11]CCO₂ concentrations in arterial plasma were determined in three dogs (total of six experiments) at 2, 5, 10, and 20 min after injection. In three human subjects venous [11]CCO₂ concentration was measured 1, 2, 4, 6, 8, 10, 20, and 30 min following injection. For this purpose 1 ml of 0.05N NaOH was added to 3 ml of blood in a heparinized tube. The mixture was immediately vortexed and a 1-ml aliquot was withdrawn and placed in a 1.5-ml centrifuge tube. After centrifugation for 5 min at 12,700 g, the radioactivity in the tube was measured in a well counter, the soluble fraction removed and the radioactivity in the pellet immediately remeasured. The soluble fraction was then applied to a gang of 3 Waters QMA SEP-PAKS that had been previously equilibrated with 0.01N NaOH. The Sep-paks were then eluted with 0.01N NaOH at the rate of 2.5 ml/min and two 5-ml fractions were taken. The amount of radioactivity contained in the combined eluant fractions (containing the ^{11}C-acetate) and in each of the SEP-PAKS (containing the ^{11}C-bicarbonate) was then determined using an auto-gamma counter. The method was validated by applying it to blood containing only [11]CCO₂ or ^{11}C-acetate. Ninety-five percent of the [11]CCO₂ was retained in the SEP-PAKS, whereas 94% of the ^{11}C-acetate was found in the eluant fraction.

Data Analysis

The three-compartmental model A (Fig. 1) was fitted to the tissue time-activity curves in the animal experiments. The solution equation to model A is given by:

$$C_{tiss}(t) = \{A_1 \exp(-(k_2 + k_3)t) + A_2 \exp(-k_4 t)\} \otimes C_a(t)\qquad\text{Eq. 4}$$

$$A_1 = K_1(1 - k_3/(k_2 + k_3))$$

$$A_2 = K_1(k_3/(k_2 + k_3))$$

where Ctiss(t) is the sum of the activity concentration in the tissue compartments and $C_a(t)$ is the ^{11}C-acetate input function. The asterisk represents mathematical convolution. The parameter k3 describes ^{11}C activity exchange between the tissue compartments, while k2 and k4 determine the transport of ^{11}C activity from the tissue compartments to blood. If, in equation 4, the parameter k4 is much smaller than the sum k2 + k3 and the acquisition time is short relative to the half-time (T½) of the
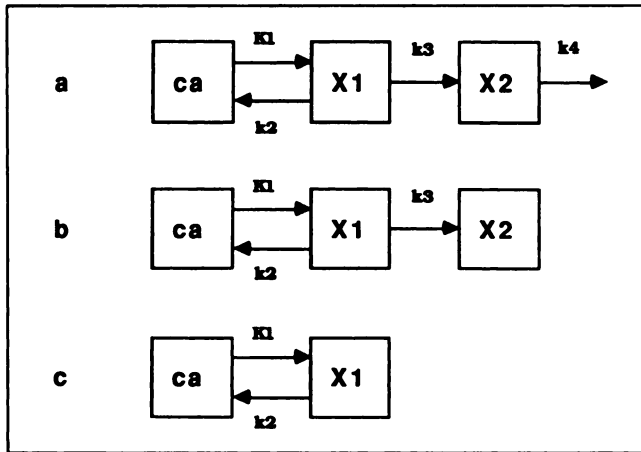
FIGURE 1. Model configurations comprising 1 and 2 tissue compartments. Ca represents arterial ^{11}C-acetate activity, x1 and x2 are tissue compartments.

second exponential ($T_{1/2} = \ln(2)/k4$), then ^{c}tiss will be adequately approximated by:

$$C_{tiss}(t) = \{A_1 \exp(-(k_2 + k_3)t) + A_2\} \otimes C_a(t) \qquad \text{Eq. 5}$$

which is the solution equation of model B (Fig. 1). A1 and A2 are defined in equation 4.

Model B and two-compartmental model C were employed to fit the human data. The solution equation of model C is:

$$C_{tiss}(t) = K_1 \exp(-k_2 t) \otimes C_a(t) \qquad \text{Eq. 6}$$

Due to the shorter acquisition time and the slower clearance rates of ^{11}C activity from myocardial tissue in the human compared to the animal studies, model A was not used to analyze the human data.

The tissue time-activity curves as measured with PET (^{c}pet) include, in addition to the tissue component [^{c}tiss(t)] activity from the vascular space and are affected by spillover of counts from tissue to blood pool and vice versa. These effects were accounted for by parameter TBV (total blood volume) as introduced in the following equation:

$$C_{PET}(t) = (1 - TBV) \, C_{tiss}(t) + TBV \, C_{tot}(t) \qquad \text{Eq. 7}$$

where $c_{tot}(t)$ represents total blood activity (ca(t) + concentration of labeled metabolites). Functional equation 8 was used to fit the data of all studies. All employed models therefore contained, besides the rate constants k, three additional parameters (a_o, m, and TBV) to be estimated by the fitting routine. In the animal and human studies, fitting was started with the first data point after arrival of the activity in the region of interest.

In addition, the exponential function:

$$y(t) = A_1 \exp(-\lambda_1 t) + A_2 \exp(-\lambda_2 t) \qquad \text{Eq. 8}$$

was fitted to the myocardial ^{11}C time-activity curves of the animal studies and the exponential functions 10 and 11 to the tissue time-activity curves of the human studies.

$$y(t) = A_1 \exp(-\lambda_c t) + A_2 \qquad \text{Eq. 9}$$

$$y(t) = A_1 \exp(-\lambda_m t) \qquad \text{Eq. 10}$$

Fitting was started with the time of onset of the most rapid decline of tracer. The exponentials λ_1 and parameter k2 of model

A were correlated with the directly measured myocardial oxygen consumption in the animal experiments. In the human studies, the exponentials λ_c and λ_m and parameter k2 of the models B and C were correlated with the rate-pressure product as indirect marker for myocardial oxygen consumption.

Computer Simulation. Variability in shape and amount of recirculating ^{11}C-acetate will lead to variability in the λ values derived from exponential fitting. This effect was directly assessed by means of a computer simulation. For this purpose simulated tissue time-activity curves of 30 min duration were generated using the input functions of all 8 human subjects and the 11 dog experiments and the models A and C. The input functions were corrected for metabolites using the following method: Equation 1 was fitted to the measured values in each experiment with metabolite measurements, yielding estimates of a_o and m. The mean of these values was then used for the metabolite correction. The exponential functions 9 and 11 were then fitted to the simulated tissue time-activity curves.

Curve Fitting Procedures and Statistical Analysis. Values were expressed as mean and standard deviation. All parameter estimations used a weighted least squares method based on the Marquart algorithm and the weights set inversely proportional to the counts acquired. Models were fitted using the differential equations and numerical integration. The model configuration A with floating metabolite correction included estimation of seven parameters, while model C employed for human studies was reduced to five estimated model parameters.
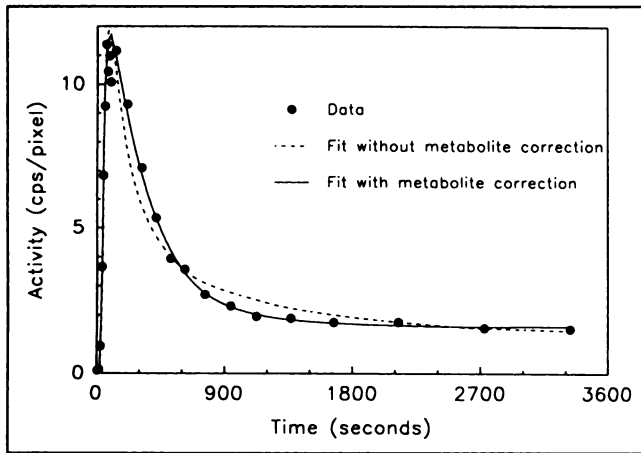
RESULTS

Animal Studies

Figure 2 shows serial cross-sectional images of a typical animal PET study. The passage of the ^{11}C activity through the right and left ventricle is seen in the first images, myocardial uptake of ^{11}C-acetate and the subsequent ^{11}C clearance are demonstrated in the second and third row of images. The corresponding tissue time-activity curve is shown in Figure 3 (closed circles). The time-activity curve is characterized by avid uptake of tracer by tissue and subsequent biexponential clearance, which results in a
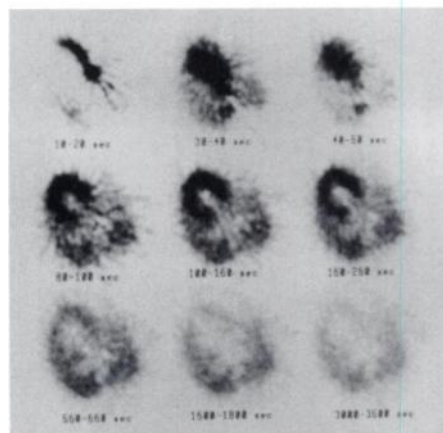
FIGURE 2. Serial cross-sectional images of a midventricular slice after intravenous injection of ^{11}C-acetate. The images initially display ^{11}C activity in right ventricular and left ventricular chambers. After uptake in the myocardium ^{11}C activity clears rapidly.

FIGURE 3. Tissue time-activity curve of a dog experiment (closed circles). Overlaid are the fitting results calculated with and without metabolite correction applied to the arterial time-activity curve. Metabolite correction was performed with the floating parameter approach.

rapid first ^{11}C clearance phase followed by slower second phase.

Validation of the Model

The model approach was validated by establishing the correlation between model derived parameter k2, calculated with model A, and directly measured myocardial oxygen consumption. Directly measured myocardial oxygen consumption ranged from 5.3 to 30.8 ml/min/100 g in the animals studied. Figure 4 describes the relationship between scintigraphic results and measured oxygen con-
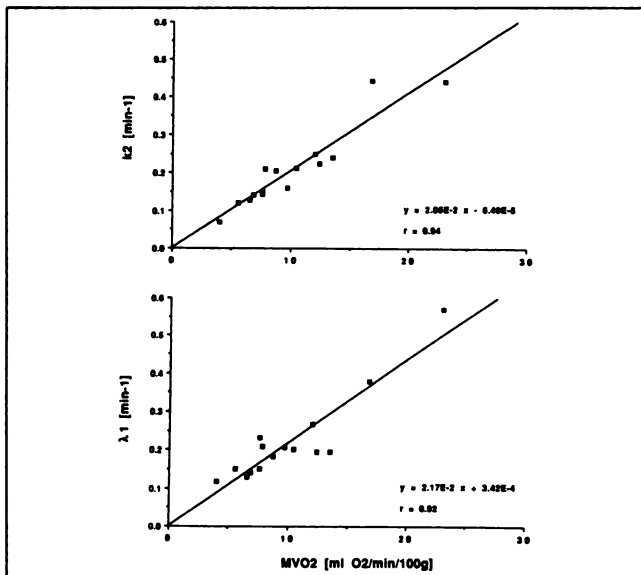

FIGURE 4. Relation between kinetic parameters and myocardial oxygen consumption (animal data, n = 15). Top panel: k2, estimated by a three-compartmental model (A). Bottom panel: $\lambda 1$, determined by fitting biexponential function y = A1 exp(−11 t) + A2 exp(−12 t) to the tissue clearance curves following injection of ^{11}C-acetate.

sumption. The top panel summarizes the k2 values of the model approach A, while the lower panel shows the results of biexponential fitting of tissue time-activity curve. Both measurements closely correlate with the reference determination of myocardial oxygen consumption (r = 0.94 and 0.92, respectively). The slope of the linear regression line to the data was similar for both methods. The regression line was slightly steeper (0.020) for biexponential fitting than that for the model approach (0.0194).

Carbon-11 Metabolites in Blood

Although these data indicate, that the use of a tracer kinetic model including metabolite correction yields close correlation with the measured oxygen consumption, we compared the measured ^{11}CCO$_2$ contamination of the input function with the prediction by the model. The need of metabolite correction for the accurate fitting of the tissue data is demonstrated in Figure 3. This example shows the fit of a tissue time-activity curve using model A with and without metabolite correction. The dotted line represents the fit without correction and deviates considerably from the PET measured data points, while the corrected fit (solid line) tightly follows the scintigraphic data. Figure 5 (top panel) shows the metabolic data obtained in 6 animal experiments as a function of time after intravenous injection. Carbon-11 CO$_2$ rapidly increased in blood and plateaued at about 65% of total ^{11}C activity at 10 min after intravenous injection. The solid line represents the time course of the metabolite fraction as calcu-
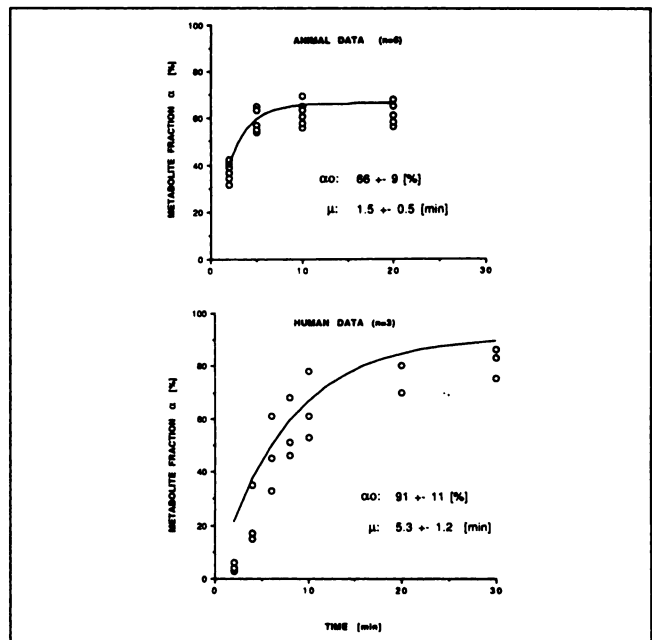
FIGURE 5. Measured metabolite fraction a (open circles) and mean continuous time course of a as derived from model (solid line). The continuous time course is described by equation a(t) = ao (1 − exp(−ln(2) t/m)). The curve was generated with the mean of the model-derived values ao and m from each experiment with metabolite measurements. Mean and standard deviation of ao and m are additionally indicated below each curve.

lated with Equation 1 and the mean of the model derived values a_o, μ.

Human Studies

Following the experimental validation in dogs, the model approach was applied to human ^{11}C-acetate PET studies. Because of the lower range of rate-pressure products in the human subjects (7,040–15,600 mmHg min-1), the tissue time-activity curves had a monoexponential appearance and were, therefore, fitted with models B and C which contained fewer parameters. Figure 6 shows the relationship between PET derived estimates of ^{11}C tissue clearance and heart rate-pressure product as indirect marker of myocardial oxygen consumption. Monoexponential fitting of the myocardial ^{11}C time-activity curves yielded a relative low correlation coefficient between clearance rate and rate-pressure product (r = 0.62 and 0.51). Please note the relative small range of rate-pressure product values in this patient population, which was studied under resting conditions only. This may explain the lower r-value of this fitting approach as compared to values reported for exercise or pharmacologic intervention studies (1,8). However, the use of a tracer kinetic model (model B) improved the prediction of myocardial oxygen demand in this data set to 0.91. The correlation coefficient for the simpler model C was lower than that of model B, but still substantially higher than the correlation determined by monoexponential fitting. Besides the correlation coefficient, the slope of the regression line was considerably steeper, when the tracer kinetic model approach was employed. Monoexponential fitting of the ^{11}C clearance rate yielded relatively less change in estimates as compared to rate-pressure changes limiting the dynamic range of the measurement.

Carbon-11 Metabolites in Blood. Figure 5 (lower panel) shows the time course of metabolite appearance in blood comparing the measured ^{11}CCO$_2$ concentration and predicted values in humans. These data show a slower rise of relative ^{11}CCO$_2$ blood content in human studies as compared to animal data (μ = 5.3 versus 1.5 min). However, ^{11}CCO$_2$ reaches a higher plateau at about 20 min as compared to the animal data (upper panel).

Effect of Input Function Variability. A computer simulation study was performed to assess the effect of variability in shape and amount of recirculating ^{11}C-acetate on the λ values derived from exponential fitting. In a first simulation, model C (K1 = 1.0, k2 = 0.1) was used to generate the human and animal tissue time-activity curves. Monoexponential fitting was then performed to these tissue curves. The result (Fig. 7A–B) demonstrates the two major effects of recirculation: (a) the λ values are lower than the model parameters k2 (λ/k2 < 1), and (b) there is a substantial degree of variation in the λ values. It is important to note that recirculation is the sole cause of both effects, since the input function represents the only variable in this simulation. Furthermore, the relative variation is substantially larger in the human λ values (20% versus 9% in the animal values). This may explain why the model approach substantially improved the correlation with the rate-pressure product in the human studies, but not with the directly measured oxygen consumption in the dog experiments. Also, the relative reduction in magnitude of the λ values was higher in the simulation with the animal data. This is consistent with the higher fraction of ^{11}C-
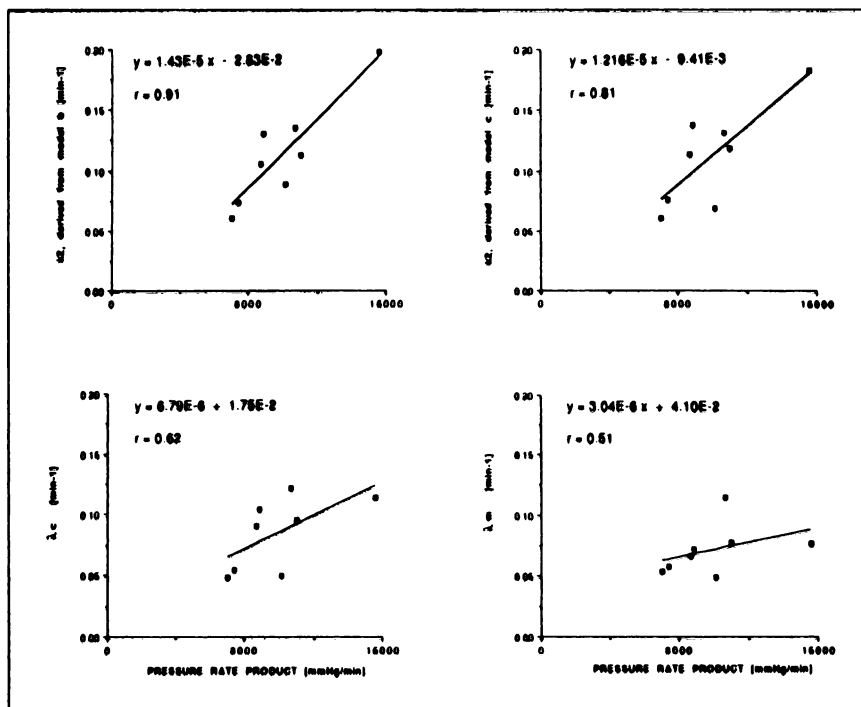
FIGURE 6. Relation between model derived parameters k2 from model B and C (top panel) and exponentials λ (bottom panel) and the rate-pressure product (human data, n = 8). Exponential λc and λm were determined by fitting of the following functions to the tissue ^{11}C clearance curves after injection of ^{11}C-acetate: y = A1 exp(−lc t) + A2 and y = A1 exp(−lm).
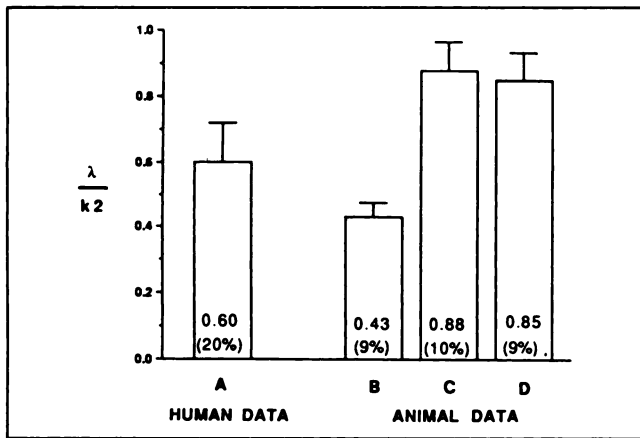
FIGURE 7. Bar graph of the λ/k2 ratio, obtained from refitting computer calculated tissue time-activity curves generated for the input functions of all human and animal experiments. In A (human input functions) and B (animal input functions), one-tissue compartment model c (k1 = 1.0, k2 = 0.1 min-1) was used to generate the simulated tissue time-activity curves. These were refitted employing the monoexponential; y = A1 exp(−λ * t). In C and D (animal input functions), the tissue time-activity curves were generated with a two-tissue compartment model, a, and different k values (C: k1 = 1.0, k2 = 0.1, k3 = 0.005, k4 = 0.001 min-1; D: kl = 1.0, k2 = 0.2, k3 = 0.01, k4 = 0.001 min-1). Refitting was performed using the biexponential: y = A1 exp(−λ1 * t) + A2 * exp(−λ2 * t).

acetate found in the tail of the input function of the animal studies. However, the slope of the regression line was similar for the k2 and the λ values in the animal experiments (Fig. 4), whereas there was a clear difference in the human studies (Fig. 6). These data suggest a larger reduction in the λ/k2 ratio in human studies, which is contrary to the simulation results. To examine this discrepancy, additional sets of animal tissue time-activity curves were generated using the three-compartmental model. One set (C) was calculated with the same k2 value used in the previous simulation (K1 = 1.0, k2 = 0.1, k3 = 0.005, k4 = 0.001). In the second set, (D) k2 and k3 were increased (K1 = 1.0, k2 = 0.2, k3 = 0.01, k4 = 0.001). Biexponential fitting was then performed to these tissue time-activity curves. These simulations showed, independent of the magnitude of k2 and k3, much less reduction in the λ/k2 ratio (Fig. 7C-D). This result suggests that the λ1 values (biexponential fitting) are considerably less affected by recirculating activity than the λm values (monoexponential fitting).

DISCUSSION

The results of this study suggest that the noninvasive estimation of myocardial oxygen consumption in human subjects by ^{11}C-acetate PET imaging can be improved by use of a compartmental model. This is most likely due to the ability of the model approach to account for recirculating ^{11}C-acetate occurring after intravenous injection of the tracer.

Kinetic Parameters and Myocardial Oxygen Consumption

Several studies have shown that the first phase of the myocardial ^{11}C clearance following intracoronary and intravenous injection of ^{11}C-acetate mirrors the production of labeled [11]CCO$_2$ by the myocardium in rats (6), rabbits (3), and dogs (2,4). This part of the clearance curve is therefore related to the flux of labeled acetate and metabolites through the tricarboxylic acid cycle (TCA cycle). The fact that the time course of the labeled activity is described well by one parameter (λ or k2) indicates that λ and k2 are closely related to the rate-limiting step of this process. Labeled and unlabeled acetyl-CoA enter the tricarboxylic acid cycle (TCA cycle) and are metabolized to CO_2. The concept of the rate-limiting step therefore links λ or k2 to the flux of unlabeled acetate through the TCA cycle. This flux in turn is directly related to oxygen consumption through a proportionality factor f which is determined by the amount of oxygen used per unit of acetyl-CoA entering the TCA cycle from the metabolic pathways feeding the cycle. As noted previously (7,11) the stoichiometry of the total oxidation of fatty acid and glucose to CO_2 and H_2O shows that f is slightly different for the two substrates (2.875 and 3.0 mol O_2 per mol acetyl-CoA respectively). Experimental work in dogs indicated that a small shift in the expected direction of the ratio λ_1/MVO$_2$ can be detected when metabolism is changed from predominantly fatty acid oxidation to glucose oxidation (7).

The Model Approach

Tracer kinetic models describe the time course of radioactivity in tissue by the kinetics of different compartments. These represent pools of labeled chemical species displaying similar kinetics and are connected through rate constants k. Parameter k2 describes the flux of activity from compartment x1 back to intravascular space (Fig. 1). Since this parameter correlates closely with oxygen consumption, it is related to the flux of acetate through the TCA cycle. Compartment x1 represents all labeled chemical species before that step. A recent study demonstrated that the main constituent of this compartment is the amino acid glutamate (to a lesser extent aspartate), and not acetate as might be assumed (12). Parameter k3 describes the production of labeled metabolites from compartment x1 which enter compartment x2. Glutamate is partially converted to glutamine, which was found to be a major component of tissue activity later in the study (12) and could therefore account for most activity in compartment x2. The absolute flux of acetate through the TCA cycle is determined by the product of k2 and the size of compartment x1. Therefore, k2 itself is proportional to the acetate flux only if the size of compartment x1 is constant. The dependence on a constant size of this metabolic compartment indicates a potential limitation of the usefulness of λ or k values as marker of oxygen consumption. However, it is remarkable that the established correlations between the λ values and MVO$_2$ were found to be stable under

various pathophysiologic conditions including ischemia (11), when myocyte metabolism may be changed (3). However, one study in isolated rat hearts demonstrated that the relationship between λ and acetate flux was considerably altered after addition of nontracer amounts of acetate to the perfusate (6), which may have changed the size of compartment x1.

The Model Approach and Exponential Fitting

In studies with intracoronary tracer injection, the tracer delivery to tissue is limited to a short time interval and the amount of recirculation of tracer is minimized. The analysis of tissue clearance curves yields direct information on the metabolic kinetics of the tracer which, for acetate, are related to tissue oxygen consumption. In this situation, the model approach leads to similar results as exponential fitting. After intravenous injection of tracer, however, recirculation is not negligible. After passage of the bolus, ^{11}C-acetate continues to enter the tissue space. This sustained influx lowers the net ^{11}C clearance from tissue. The model approach, by inherently performing a deconvolution, corrects for recirculation. In contrast, exponential fitting will lead to slower clearance rates. This effect is more pronounced when monoexponential fitting is employed as suggested by the computer simulation performed in this study. Furthermore, the amount of influx, which is related to the time course of recirculation, can be expected to vary between studies. This may be especially true in pathological conditions with altered blood volume and/or cardiac output. This variation of tracer delivery introduces errors in the estimation of absolute oxygen consumption employing exponential fitting of tissue kinetics, which consists of comparing the λ values to a calibration curve established in dog experiments.

The advantage of the exponential fitting approach is clearly its simplicity. In contrast, the model approach requires the definition of an input function and the introduction of three additional parameters for the correction of ^{11}C metabolites and spillover effects. The increased complexity potentially introduces errors. This disadvantage of the model approach has to be weighed against its ability to take recirculating activity into account. It can be expected that the model approach yields more consistent estimates of MVO2 than exponential fitting especially in situations with short acquisition time and increased input function variability. This was confirmed by our finding that the model approach yielded higher correlation values in the human experiments where the tissue clearance curve appeared monoexponential and the input functions displayed more variability than in the animal experiments.

The choice of the most appropriate model represents an important consideration. Basically, tissue clearance after injection of ^{11}C-acetate is at least biexponential. However, under resting conditions with low cardiac work, tissue clearance of ^{11}C activity is relatively slow. Under these conditions the accurate estimation of the parameters of a two-tissue compartment model (for instance model A) would require long acquisition times. This is clinically impractical and problematic due to the relatively short physical half-life of ^{11}C (20 min). One therefore has to resort to simplified models (or mono- as opposed to biexponential fitting). In the range of work loads examined in the human experiments of this study and the acquisition time of 40 min, the simplified three-compartmental model B yielded the best results. However, it is important to note, that the estimate of myocardial oxygen consumption from model-derived k2 values, requires a calibration curve established with the same model approach in order to convert k2 in absolute values of oxygen consumption.

Methods of Metabolite Correction

The separation of labeled metabolites in blood from ^{11}C-acetate is needed for the definition of the arterial ^{11}C-acetate input function. As shown in Figure 3, tissue time-activity curves can only be accurately fitted if the input function is corrected for ^{11}CCO$_2$. The direct measurement of ^{11}C metabolites would be desirable, but such determinations are impractical in clinical studies. The results of this study suggest that the metabolite correction can be performed with a mathematical method in close agreement with measured values, which obviates the need for direct metabolite measurements in plasma. Such approach clearly facilitates the application of the model approach in a clinical setting. However, further studies are required to validate this method under pathophysiologic conditions.

SUMMARY

This study suggests that the model approach, mainly by accounting for recirculating ^{11}C-acetate, allows a more consistent estimation of absolute regional myocardial oxygen consumption with ^{11}C-acetate and PET in human subjects. However, a correction for labeled metabolites in blood appears necessary and can be performed by a mathematical method. We conclude that the model approach may prove useful in the clinical evaluation of regional myocardial oxygen consumption by PET.

ACKNOWLEDGMENTS

REFERENCES

1. Armbrecht JJ, Buxton DB, Brunken RC, Phelps ME, Schelbert HR. Regional myocardial oxygen consumption determined noninvasively in humans with [1-^{11}C] acetate and dynamic positron tomography. *Circulation* 1989;80:863–72.

2. Armbrecht JJ, Buxton DB, Schelbert HR. Validation of [1-¹¹C] acetate as a tracer for noninvasive assessment of oxidative metabolism with positron emission tomography in normal, ischemic, postischemic, and hyperemic canine myocardium. *Circulation* 1990;81:1954–1605.

3. Brown M, Marshall DR, Sobel BE, Bergmann SR. Delineation of myocardial oxygen utilization with carbon-11-labeled acetate. *Circulation* 1987;76:687–96.

4. Brown MA, Myears DW, Bergmann SR. Noninvasive assessment of canine myocardial oxidative metabolism with carbon-11-acetate and positron emission tomography. *J Am Coll Cardiol* 1988;12:1054–1063.

5. Brown MA, Myears DW, Bergmann SR. Validity of estimates of myocardial oxidative metabolism with carbon-11-acetate and positron emission tomography despite altered patterns of substrate utilization. *J Nucl Med* 1989;30:187–93.

6. Buxton DB, Schwaiger M, Nguyen A, Phelps ME, Schelbert HR. Radiolabeled acetate as a tracer of myocardial tricarboxylic acid cycle flux. *Circ Res* 1988;63:628–34.

7. Buxton DB, Nienaber CA, Luxen A, Ratib O, Hansen H, Phelps ME, Schelbert HR. Noninvasive quantitation of regional myocardial oxygen

consumption in vivo with [1-¹¹C] acetate and dynamic positron emission tomography. *Circulation* 1989;79:134–42.

8. Henes CG, Bergmann SR, Walsh MN, Sobel BE, Geltman EM. Assessment of myocardial oxidative metabolic reserve with positron emission tomography and carbon-11-acetate. *J Nucl Med* 1989;30:1489–99.

9. Heyman M, Payne B, Hoffman J, Rudolph A. Blood flow measurements with radionuclide-labeled particles. *Prog Cardiovasc Dis* 1977;20:55–79.

10. Gambhir SS, Schwaiger M, Huang SC, Krivokapich J, Schelbert HR, Nienaber CA, Phelps ME. Simple noninvasive quantification method for measuring myocardial glucose utilization in humans employing positron emission tomography and fluorine-18-deoxyglucose. *J Nucl Med* 1989;30:359–66.

11. Randle PJ, England PJ, Denton RM. Control of the tricarboxylate cycle and its interactions with glycolysis during acetate utilization in rat heart. *Biochem J* 1970.

12. Ng C, Huang HR, Schelbert HR, Buxton DB. A kinetic model for C-11-acetate as a tracer for myocardial oxidative metabolism. *J Nucl Med* 1990;31:1581.

EDITORIAL

Relationship Between Myocardial Clearance Rates of Carbon-11-Acetate-Derived Radiolabel and Oxidative Metabolism: Physiologic Basis and Clinical Significance

APPROACHES TO IMAGING MYOCARDIAL METABOLISM

Unlike the brain, which normally utilizes glucose as its primary metabolic substrate, the heart relies on a variety of substrates for energy production. In fact, under baseline conditions, glucose metabolism accounts for only about half of all cardiac substrate metabolism, and this value can decrease with decreases in blood-glucose levels. Therefore, while fluorodeoxyglucose (FDG), a glucose analog, is the standard tracer for quantifying cerebral metabolism and for imaging cerebral function with PET, it cannot be used to estimate cardiac energy production. Even the regional patterns of FDG-derived radiolabel accumulation do not necessarily reflect the patterns of regional cardiac energy production qualitatively (*1–3*).

Researchers have therefore had to seek other potential metabolic tracers in efforts to find a method of imaging metabolism in the heart. For example, radiolabeled fatty acids have been ex-

plored as metabolic tracers, but fatty acid metabolism accounts for only 40%–80% of overall cardiac energy production under normal conditions and is highly variable. Radiolabeled molecular oxygen has been used to image brain oxidative metabolism, but technical difficulties have prevented its use in the heart.

Recently, the use of some radiolabeled analogs of acetate has been suggested as an approach to image myocardial oxidative metabolism. Acetate is rapidly converted into acetylcoenzyme A (acetyl CoA) in the heart and acetyl CoA is the link between Krebs cycle oxidative metabolism and the initial metabolism of glucose, fatty acids, lactate, and protein. The possibility of using an acetate analog to map overall oxidative metabolism is therefore inviting.

Interestingly, the relationship between acetate and its fluorinated derivative, fluoroacetate, at first resembles that of glucose and fluorodeoxyglucose. FDG is metabolized to FDG-6-phosphate as glucose is metabolized to glucose-6-phosphate, but further FDG-6-phosphate metabolism is very slow and therefore it accumulates in proportion to the rate of glucose me-

tabolism (*4,5*). Similarly, fluoroacetate is metabolized to fluorocitrate as acetate is metabolized to citrate, with further metabolism of fluorocitrate being extremely slow. Unfortunately, the analogy ends here. Fluoroacetate kinetics are very different from acetate kinetics (*6*), and fluorocitrate is an extremely potent metabolic poison. Thus, fluoroacetate has not found use as a metabolic tracer.

RADIOLABELED ACETATE AS A METABOLIC TRACER

Investigators have had better luck with the use of radiolabeled acetate (ACE) itself as a metabolic tracer. Following intravenous administration, ACE is converted into ACE-CoA in heart cells by a rapid and poorly regulated process (*7,8*). The ACE-CoA is subsequently metabolized through the Krebs cycle with the radiolabel being lost as CO_2. Because ACE can be labeled with positron-emitting ¹¹C, and because regional cardiac ¹¹C activity over time can then be imaged with PET scanners, the use of ¹¹C-ACE in PET imaging of cardiac metabolism has been investigated.

Preliminary studies suggested an